Paper H :

Simulation of Brake Block Induced Corrugation on Railway Wheels

Ulf Sellgren

(8th Int. ANSYS Conference, August 17-19, Pittsburgh, PA, 1998)

Simulation of Brake Block Induced Corrugation on Railway Wheels

Ulf Sellgren
Department of Machine Design, Royal Institute of Technology (KTH), Stockholm, Sweden

ABSTRACT

Railway wheels that are equipped with cast-iron brake blocks generate significantly more rolling noise than wheels with other types of braking devices or block materials. The roughness of the treads on cast-iron block-braked wheels has typically a peak at a wavelength around 6 cm. The complex interaction between quasi-static and dynamic mechanical behavior and thermal, chemical, and metallurgical effects in the block-wheel contact combined with the rolling and sliding situation in the wheel-rail contact has made it difficult to get an understanding of the causes from field measurements. Coupled transient thermal and quasi-static mechanical FE simulations with ANSYS show that thermoelastic instability (TEI) may be a major cause for the roughness initiation.

NOMENCLATURE

A_n nominal contact area (m^2)
$^e\mathbf{C}$ damping matrix (Ns/m)
$^t\mathbf{C}$ specific heat matrix (J/K)
c specific heat (J/kgK)
$C_{N,T}$ spatial correlation between nodal temperature and normal contact forces
E Young's modulus (Pa)
$E^* = \left(\frac{1-\nu_1^2}{E_1} + \frac{1-\nu_2^2}{E_2} \right)^{-1}$ composite Young´s modulus (Pa)
$^t\mathbf{F} = E\alpha(\mathbf{T} - \mathbf{T_0})$ nodal force in mechanical domain (N) due to a temperature field
h thickness of the surface layer worn off (m)
$\mathbf{M}$ mass matrix (kg)
$^e\mathbf{K}$ stiffness matrix (N/m)
k thermal conductivity (W/mK)
K a dimensionless wear constant
N normal force acting on the contact area (N)
$Pe = \frac{v \cdot 2R}{4\kappa}$ the Peclet number, a dimensionless heat source motion number
$\mathbf{Q}$ rate of heat generated (W)
$^e\mathbf{Q} = \mu \mathbf{N} v$ heat rate due to friction between bodies in sliding contact (W)
$q, \bar{q}$ heat flux and mean heat flux per unit area (W/m^2)

R the radius of a circular contact surface
R_ς autocorrelation between nodal temperature and normal contact forces
$2s_v$ length of an elliptical contact zone in the sliding dir. (m)
$\mathbf{T}$ nodal temperature vector (K)
$\mathbf{T}_0$ the stress free temperature (K)
t, Δt simulation time and time step (s)
$\mathbf{u}$ nodal DOF displacement vector (m)
v , v_c sliding velocity and critical sliding velocity (m/s)
w , w_c wear coefficient and critical wear coefficient (PA^{-1})
W volume loss due to sliding wear (m^3)

δ the conducting length of an element
δ_s the length of a contact element in the sliding direction
ρ density (kg/m^3)
μ coefficient of friction
α coefficient of thermal expansion (1/K)
λ wavelength for a sine-shaped perturbation (m)
λ_{max} the largest thermal eigenvalue
ν Poissons ratio
$\kappa = \frac{k}{\rho c}$ thermal diffusivity (m^2/s)
$\sigma = (1+\nu)\alpha / k$ the ”distortivity” of the material (m/W)
φ local coord. in the sliding direction along block (m)
θ local coord. in the sliding dir. along wheel segment (m)
Ψ heat partitioning factor

INTRODUCTION

Freight wagons are traditionally equipped with block brakes that operate on the wheel tread (see figure 1). The most commonly used block material is cast iron, but also sinter and composition materials are in use. Blocks made of cast iron are relatively cheap to manufacture. They have also a positive influence on the adhesion between wheel and tread, by increasing the micro-roughness of the wheel tread. An increased adhesion has a positive influence on braking as well as on traction. This is also the main reason why disc brakes on modern trains often are complemented with cast iron block brakes.

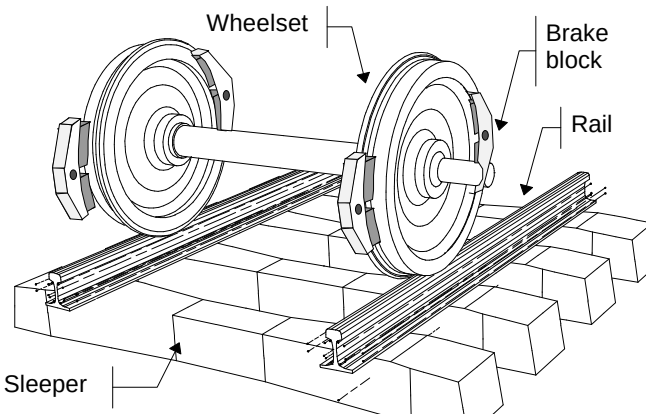

Figure 1. A wheelset equipped with block brakes.

Irregularities with a wavelength that is of the same order as the length of the contact patch between wheel and rail, or longer, cause excessive vibration and thus sound radiation from both the wheelsets and the track (Thompson, 1994). Figure 2 shows the measured roughness of block-braked wheels of NS rolling stock (Dittrich et al., 1994) and the rail roughness on the Dutch network (Dings 1994). The roughness growth on cast-iron block-braked wheels is characterized by three phases - initiation, propagation, and finally a steady-state phase when the wear rate is uniform in the circumferencial direction, i.e. the roughness does not increase with time. Dittrich et al. (1994) reported that the propagation phase is usually very short - just a few brake applications.

Roughness measurements have been performed by several European railroad companies over the years. They have all reported the same typical results, but they have not been able to describe the process nor to clarify the cause of the problem. The fact that there is a correlation in the 4 cm to 8 cm wavelength band between the roughness on cast-iron block-braked wheel treads and the treads on rough rail has also caused some confusion. There has though been a general opinion among experts that many types of effects and interactions contribute to the roughness initiation process. A common view has been that a high frequency dynamic behavior cause an irregular thermomechanical behavior with a slower time scale, that influence a long term irregular wear process between block and wheel.

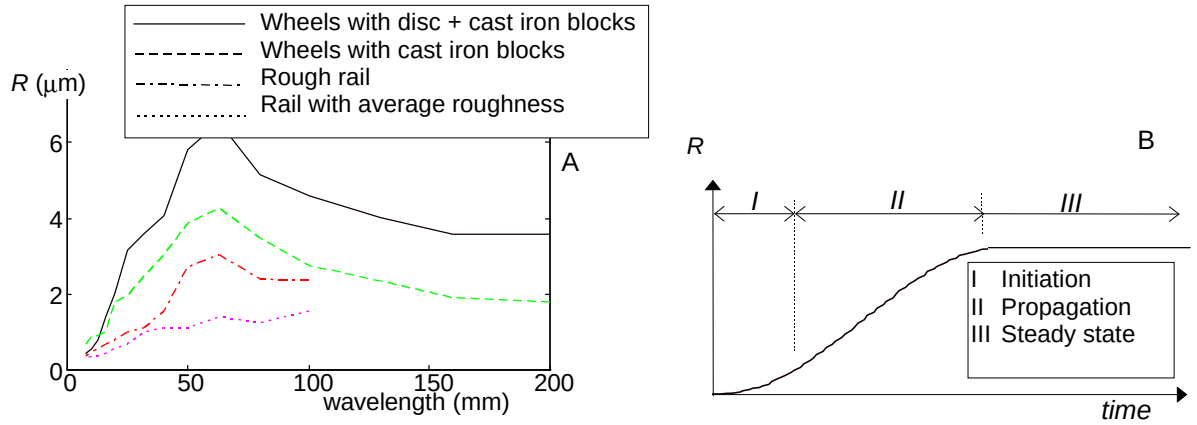

Figure 2. The typical wheel roughness is developed in three phases.

The complex interaction between mechanical and thermal behavior, and chemical and metallurgical phenomena in the block-wheel contact, combined with the severe rolling and sliding situation in the wheel-rail contact has made it very difficult to base an understanding of the transformation of the tread on results from field measurements. Vernersson (1997) demonstrated with 2D FE simulations of drag braking, where he averaged the block-wheel interaction over the wheel circumference, that an initially conform block-wheel contact in a relatively short time was transformed to a two-patch contact, i.e. the minimum number of contact points required to satisfy mechanical equilibrium, due to thermoelastic instability (TEI) effects. The presented study was performed to investigate if this effect is strong enough to develop during sliding over a single contact patch and if any correlation to the observed 6 cm roughness wavelength can be found. The TEI phenomena at braking between a standard cast iron UIC250 block and a standard UIC/ORE 1002 freight wheel with a diameter of 0.92 m, has been studied with the ANSYS 5.2 coupled simulation capability.

THERMO-ELASTIC BEHAVIOR BETWEEN BODIES IN FAST SLIDING CONTACT

The frictional heat rate, at any point in sliding contact, and at any given point in time *t*, is:

$$q_t = \mu_t \cdot p_t \cdot v_t \tag{1}$$

The portion of the heat rate that diffuses into two bodies in contact can be defined by a heat partitioning factor Ψ, such as $q_t^1 = \psi q_t$ and $q_t^2 = (1-\Psi)q_t$. The heat partitioning is influenced by the actual temperature fields in the two bodies during the sliding history. It is thus not a constant but a function of the actual temperature and contact state. The effect on the temperature field in the interacting bodies, caused by the dissipated heat, can be separated into bulk effects and surface effects. The bulk temperature is the global temperature in a body. The surface temperature is the local temperature on an interacting surface. The local temperatures that arise in the real contact areas between the contacting asperities is sometimes referred to as the flash temperature. The flash temperatures are frequently in the same order as the melting temperature of the material. Since the distinction between surface and flash temperature is not quite obvious, the local effects are referrered to as surface effects further on.

The Peclet number *Pe*, is frequently used to distinguish between slow moving contacts and fast moving contacts. For fast moving contacts, i.e. when $Pe > 5$ (Guha and Chowdhuri, 1996), very high surface temperatures can be observed. Archard (1959) proposed that with constant mean heat flux $\bar{q}$, the surface temperature at fast moving contact, as a function of time *t*,, could be written:

$$T(t) = \frac{2\bar{q} \cdot t^{0.5}}{(\pi \cdot k \cdot \rho \cdot c)^{0.5}} \tag{2}$$

where $\bar{q} = \mu \cdot \bar{p} \cdot v = \mu \frac{N}{A_n} v$ (3)

Tian and Kenedy (1994) showed that the average and maximum mean surface temperature caused by a circular and constant heat source is :

$$\bar{T} = \frac{0.61 \cdot 2R \cdot \bar{q}}{k\sqrt{\pi(0.675 + Pe)}} \tag{4}$$

$$\hat{T} = \frac{2R \cdot \bar{q}}{k\sqrt{\pi(1.273 + Pe)}} \tag{5}$$

Determination of proper values for the heat partitioning factor is crucial in any simulation of the thermal behavior at sliding contact. Archard (1959) proposed an elegant solution on that problem. His suggestion was to supply all frictional heating *q* to each of the two surfaces and then calculate the resulting temperature at the two surface, i.e. T_1 and T_2. The contact temperature *T* could now be determined from the following expression:

$$T = \left(T_1^{-1} + T_2^{-1}\right)^{-1} \tag{6}$$

The relation between T_1, T_2, and *T* can be used to calculate an explicit heat partitioning factor.

Under severe conditions of sliding between surfaces with a roughness in a microscopic scale, stationary or slowly moving hot spots of a macroscopic scale can take place (Dow and Burton, 1971). This phenomenon, which often is referred to as thermoelastic instability (TEI), was

early investigated experimentally and analytically by Barber, e.g. (Barber, 1967), and it was studied in detail by Burton (1980). TEI can occur in lubricated as well as dry contact and it is influenced by material properties, cooling, macroscopic constraints on the contacting bodies and wear (Burton, 1980).

TEI can be described as follows. A small initial sinusoidal undulation of wavelength λ will result in a fluctuation of the contact pressure with the same wavelength as the undulation. Consequently, the frictional heating will also fluctuate, which results in hot spots on regions of the surface where the pressure is further increased due to an elevated thermal expansion. As the sliding velocity approaches a critical value v_c given by

$$v_c = \frac{4\pi}{\sigma\mu E^* \lambda} \tag{7}$$

the fluctuation in pressure increases rapidly in magnitude and there is a transition from continuous to discontinuous contact, with a critical contact width that approximately is (Johnson, 1994):

$$2a_c \approx \frac{\lambda}{2\pi} \tag{8}$$

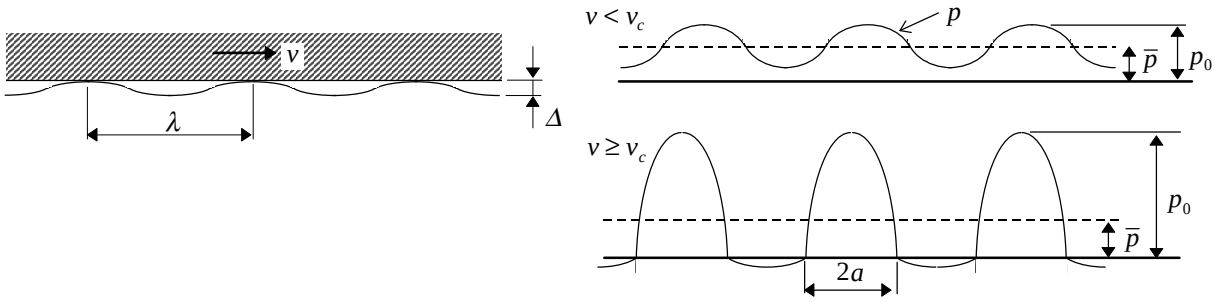

Figure 3. Thermoelastic instability gives discontinuous contact when $v > v_c$

We can reformulate equation 4 to get a critical wavelength at a given velocity:

$$\lambda_c = \frac{4\pi}{\sigma\mu E^* v} \tag{9}$$

For ordinary steel sliding at 60km/h is above the all wavelengths that are in the mm range are critical according to equation 9.

Analytical expressions for the thermally induced steady state corrugation u_z have been given, see for example (Johnson, 1994):

$$\hat{u}_z = \frac{\sigma\mu v p^* \lambda^2}{4\pi} \tag{10}$$

where $p^* = \bar{p}\left(\frac{\pi E^* \Delta / \lambda \bar{p}}{1 - \sigma\mu v E^* \lambda / 4\pi}\right)$

WEAR

Archard (1953) postulated a model for adhesive sliding wear:

$$\frac{W}{s} = K\frac{N}{H} \tag{11}$$

where *N/H* is the real contact area between the interacting asperities and *K* is a dimensionless wear constant. A popular generalization of Archards wear model is based on the assumption that the wear rate at any point on a tribological surface is proportional to the pressure and to the relative tangential velocity. If we integrate we get the thickness *h* surface layer worn off at any given point:

$$h = wps \tag{12}$$

where the wear coefficient *w* is a function of the material combination, surface topography, temperature, lubrication, etc, and it has the dimension Pa^{-1}. From equation 12 we can get the wear rate:

$$\dot{h} = wpv \tag{13}$$

Dow and Burton (1971) stated that wear can have a damping effect on the growth rate of a perturbation. Burton (1980) showed that for a conductor sliding on an insulator, instabilities will not occur for finite sliding speed if the wear coefficient is larger than a critical wear coefficient w_c defined as:

$$w_c = 2\alpha\mu\kappa/k \tag{14}$$

APPLICATION OF THE THE FINITE ELEMENT METHOD

When two physical phenomena, such as thermal behavior and elastic behavior, are closely interrelated, a coupled field simulation is usually required. In the finite element method, two common methods to couple physical domains is matrix coupling and load vector coupling respectively. In ANSYS 5.2, a coupled thermoelastic simulation capability based on load vector coupling is available (ANSYS, 1995). The equilibrium equations for the coupled thermoelastic domain is:

$$\begin{bmatrix} \mathbf{M} & \mathbf{0} \\ \mathbf{0} & \mathbf{0} \end{bmatrix} \begin{Bmatrix} \mathbf{u} \\ \mathbf{T} \end{Bmatrix} + \begin{bmatrix} {}^{e}\mathbf{C} & \mathbf{0} \\ \mathbf{0} & {}^{t}\mathbf{C} \end{bmatrix} \begin{Bmatrix} \mathbf{u} \\ \mathbf{T} \end{Bmatrix} + \begin{bmatrix} {}^{e}\mathbf{K} & \mathbf{0} \\ \mathbf{0} & {}^{t}\mathbf{K} \end{bmatrix} \begin{Bmatrix} \mathbf{u} \\ \mathbf{T} \end{Bmatrix} = \begin{Bmatrix} {}^{e}\mathbf{F} \\ {}^{t}\mathbf{Q} \end{Bmatrix} + \begin{Bmatrix} {}^{t}\mathbf{F} \\ {}^{e}\mathbf{Q} \end{Bmatrix} \tag{15}$$

High frequency dynamic scatter might severely pollute a numerical solution of a TEI dominated behavior, and make any interpretation of the simulated history very difficult. In ANSYS 5.2, time integration effects for the elastic domain can be turned off by issuing the solution command *timint,off,struc* and the coupled set of equations can thus be reduced to quasistatic form for the elastic domain, while maintaining a fully transient thermal domain:

$$\begin{bmatrix} \mathbf{0} & \mathbf{0} \\ \mathbf{0} & {}^{t}\mathbf{C} \end{bmatrix} \begin{Bmatrix} \dot{\mathbf{u}} \\ \dot{\mathbf{T}} \end{Bmatrix} + \begin{bmatrix} {}^{e}\mathbf{K} & \mathbf{0} \\ \mathbf{0} & {}^{t}\mathbf{K} \end{bmatrix} \begin{Bmatrix} \mathbf{u} \\ \mathbf{T} \end{Bmatrix} = \begin{Bmatrix} {}^{e}\mathbf{F} \\ {}^{t}\mathbf{Q} \end{Bmatrix} + \begin{Bmatrix} {}^{t}\mathbf{F} \\ {}^{e}\mathbf{Q} \end{Bmatrix} \tag{16}$$

Simulation of physical instability, such as TEI, require that the errors in the model are properly assessed. Errors introduced by an inadequate time step or a too coarse discretization and means to control these errors are discussed below.

Time step considerations

The generalized trapezoidal rule is based on the assumption that two temperature states have the relation:

$$\mathbf{T}_{t+\Delta t} = \mathbf{T}_t + \left\{(1-\beta)\dot{\mathbf{T}}_t + \beta\dot{\mathbf{T}}_{t+\Delta t}\right\}\Delta t \tag{17}$$

where β is a constant ($0 \le \beta \le 1$). For $\beta = 0$ we have an explicit formulation, and for $\beta > 0$ the formulation is implicit. By rewriting equation (16), based on equation (17), the nodal temperatures at time $t + \Delta t$ can be solved by direct integration:

$$\left(\frac{1}{\Delta t}\mathbf{C} + \beta\mathbf{K}\right)\mathbf{T}_{t+\Delta t} = \left(\frac{1}{\Delta t}\mathbf{C} - (1-\beta)\mathbf{K}\right)\mathbf{T}_t + (1-\beta)\mathbf{Q}_t + \beta\mathbf{Q}_{t+\Delta t} \tag{18}$$

Depending on β, the time step has an upper limit if the algorithm is to be numerically stable. If $\beta < 0.5$ the largest Δt for stability is:

$$\Delta t_{cr} = \frac{2}{(1-2)\lambda_{max}} \tag{19}$$

For forward difference or Euler integration, i.e. β=0, the stability limit is (Hughes, 1977):

$$\Delta t_{cr} = \frac{\delta^2}{4\kappa} \tag{20}$$

Equation (20) for three generic materials at room temperature is plotted in figure 4.

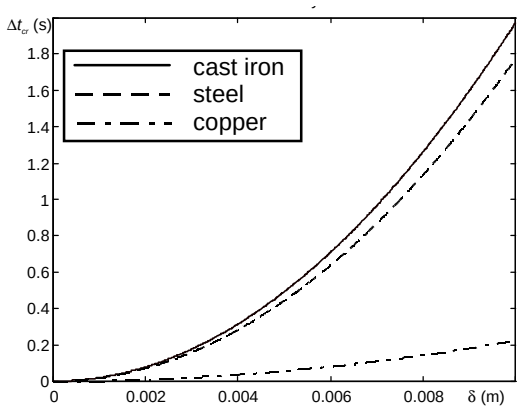

Figure 4. Critical time step for generic cast iron, steel, and copper as a function of the conducting length.

For $\beta \ge 0.5$, the integration algorithm is unconditionally stable. The most frequently used implicit scheme is the implicit central difference or the Crank-Nicholson method, which uses $\beta = 0.5$. It is unconditionally stable, but sharp transients may induce numerical oscillations in the solution. Donea (1977) showed that the Galerkin method, i.e. $\beta = 2/3$, yields better accuracy for fast-varying boundary conditions. If the problem is nonlinear, the only unconditionally stable scheme is where $\beta = 1$, i.e. the backward difference scheme, which is not particularly accurate (Hughes, 1977). To avoid undesired inaccuracies caused by numerically induced oscillations in a general nonlinear solution, it is thus necessary to take very small time steps (Rources and Alarcon, 1983).

If we want to simulate TEI between sliding surfaces, a realistic constraint on the time step is that the sliding distance over a single time step should not be larger than the length of one contact element in the sliding direction:

$$\Delta t \le \delta_s / v \tag{21}$$

An upper limit for the time step, according to equation 21 is plotted in figure 5. Plotted is also the critical time step for a cast iron material. We may refer to equation 20 as the diffusivity criterion and equation 21 as the velocity criterion. If we put equations 20 and 21 equal, we get:

$$\delta = 4\kappa / v \tag{22}$$

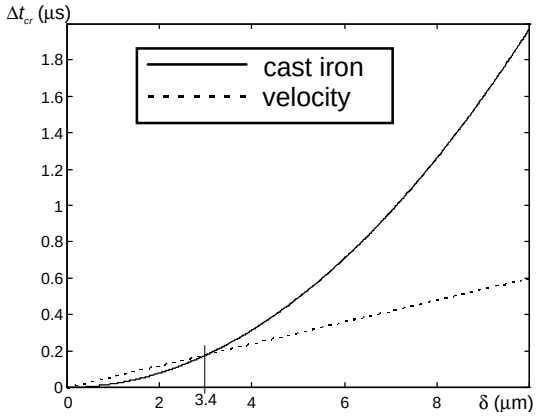

Figure 5. Maximum time step as a function of the element length at 60 km/h.

For generic cast iron and a sliding velocity of 60 km/h, equations 20 and 22 gives an element length $\delta \approx 3.4$ μm and a time step of 0.2 μs (see figure 5). For a finer discretization the maximum time step is limited by the diffusivity criterion. For a coarser discretization the velocity criterion limits the time step.

Discretization error due to linearization of a curved boundary

General contact in ANSYS is preferrably modeled with the CONTAC48 or CONTAC49 elements, which are linear isoparametric 2D and 3D elements, respectively. Discretization of a curved boundary with linear isoparametric elements introduces a geometric error (see figure 6). For a cylinder with radius r, a typical element length δ_s gives a maximum radial error:

$$\Delta r = r\left(1 - \cos\left(a\sin\left(\frac{\delta_s}{2r}\right)\right)\right) \tag{23}$$

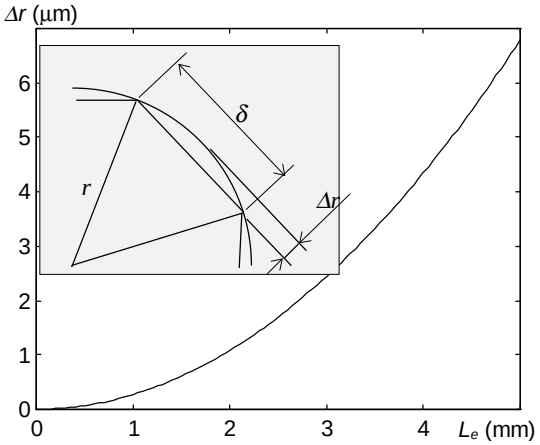

Figure 6. Radial discretization error according to eq. 22 for a radius of 0.46m.

Severe oscillation in the contact pressure, due to the polygon effect, has to be smoothed, e.g. each point can be averaged with the pressure at the two neighboring points. Such smoothing is further on is referred to as three-point smoothing:

$$p_{3p} = \left(p_{i-1} + p_i + p_{i+1}\right)/3 \tag{24}$$

Smoothing based on averaging introduces an error in the estimated peak values. An useful error value is the relative deviation from the theoretical peak value:

$$\varepsilon = \left(\hat{p}_{3p} - \hat{p}_{exact}\right)/\hat{p}_{exact} \tag{25}$$

By varying the position of a perturbation relative to the position of the discrete nodal points where the pressure is evaluated, upper and lower limits of the amplitude error defined by equation 25 can be found. Figure 7 shows the upper and lower limits of the relative error ε for a sine shaped perturbation as a function of the number of element segments per half wavelength. For 10 elements per half wavelength the error is between 3.3% and 4.5 %, and for five elements it is between 12.7% and 17%. When the wavelength is getting shorter than the length of about five elements, the error increases dramatically and the amplitude for the smoothed pressure gives a highly underestimated value for the real maximum pressure.

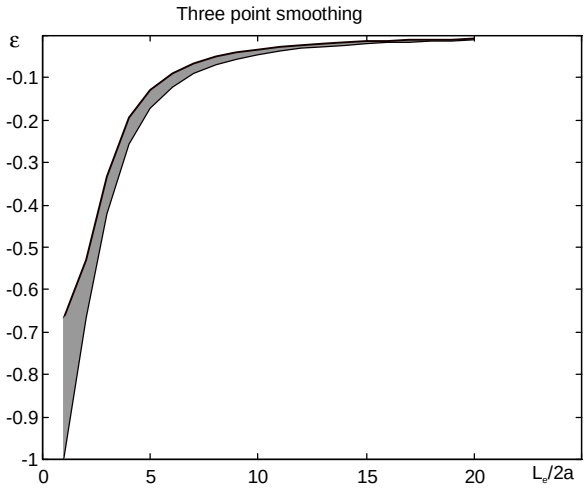

Figure 7. Upper and lower error bounds for three point smoothing.

FE MODELING

The wheel and block used in the simulations is a standard UIC/ORE 1002 wheel with a diameter of 0.92 m, which is a typical freight wheel, and two standard UIC250 blocks made of cast iron (see figure 8). Figure 9 from a static 3D FE contact simulation shows two localized pressure regions between a new block and a new wheel. The discontinuous contact is due to the doubly curved shape of the wheel tread. Quasi-static FE analysis of the 3D contact state gives valuable knowledge of the shape and size of the apperant contact area and the actual pressure distibution.

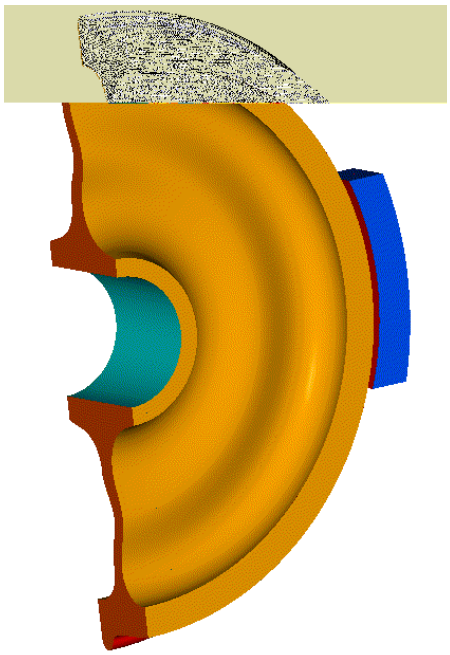

Figure 8. A symmetrical half of a UIC wheel equipped with two brake blocks.

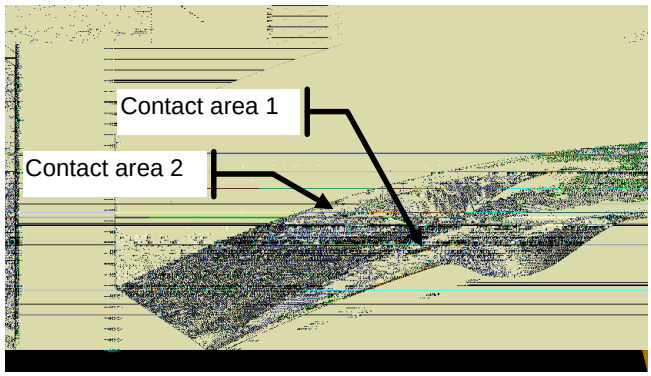

Figure 9. Contact pressure between a new block and a wheel visualized with the data surface capability in I-DEAS Master Series.

For cast iron sliding at a relative velocity of 60 km/h and a typical discretization length of 1 mm in the contact area we get a maximum integration time step of 60 μs from equation 26, which correspond to approximately 1500 DOFs for the nominal 2D block-wheel interface. The sliding distance will also considerably extend the wheel surface that has to be discretized. The thickness of the contact surface that has to be modeled further increase the size of the model with at least one order. A 3D interface model with the same level of discretization would result in 165 kDOFs just for the immediate interface model. To simulate a full 3D TEI behavior with the FE method would thus require extraordinary computer resources. The selected approach was to conduct coupled 2D simulations with FE models of one block, a block holder and a part of the wheel (see figures 10).

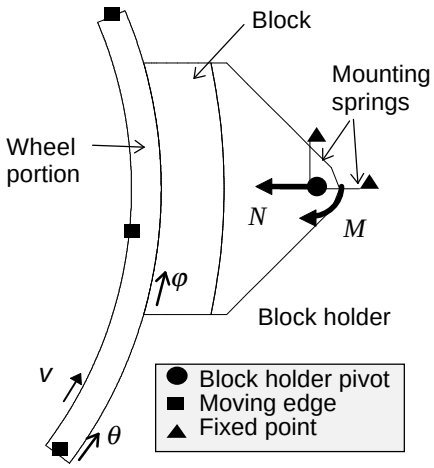

Figure 10. 2D FE model of block, holder, a portion of the wheel, and springs.

The geometric regions were discretized with the ANSYS PLANE13 element (see figure 11). The block holder pivot was spring-mounted to the surrounding world with the COMBIN14 element. The kinematic relation between block and wheel was modeled as an unsymmetric contact with the ANSYS general 2D contact element CONTAC48. The frictional forces in the contact was not considered, i.e $\mu=0$ for the contact elements, but a reaction torque M caused by the total friction force was applied at the block holder pivot.

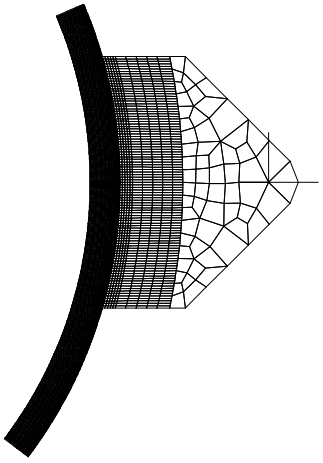

Figure 11. The Actual Discretization.

The basic modeling and simulation approach can be described as follows:

- Model cast iron block and steel block holder as is, and a portion of a steel wheel.
- Use temperature dependent material data.
- Gross sliding between block model and wheel model with prescribed displacements of the wheel boundary.
- Apply full normal brake force N and frictional reaction moment M on block holder pivot.
- Solve a coupled quasistatic mechanical and transient thermal time step.
- Get nodal contact forces from miscellaneous element data distribution between block and with user macro and smooth the distribution of the contact forces.
- Calculate nodal frictional heat rate and load nodes "in contact" with user macro.
- Rotate the wheel a sliding increment with user macro.
- Calculate incremental wear for the contact nodes and move them with the calculated wear increment normal to the target plane with user macro.

• Restart and solve a new time step.

The simulation part of the approach is briefly presented in figure 12. The face nodes for each submodel are grouped and treated as interface objects. Pairs of such interface objects with a mating relation are then coupled with constraint equations or with contact elements accordingly. Mating of face objects and environment has also been used to create boundary conditions. This approach is briefly discussed in (Sellgren, 1997).

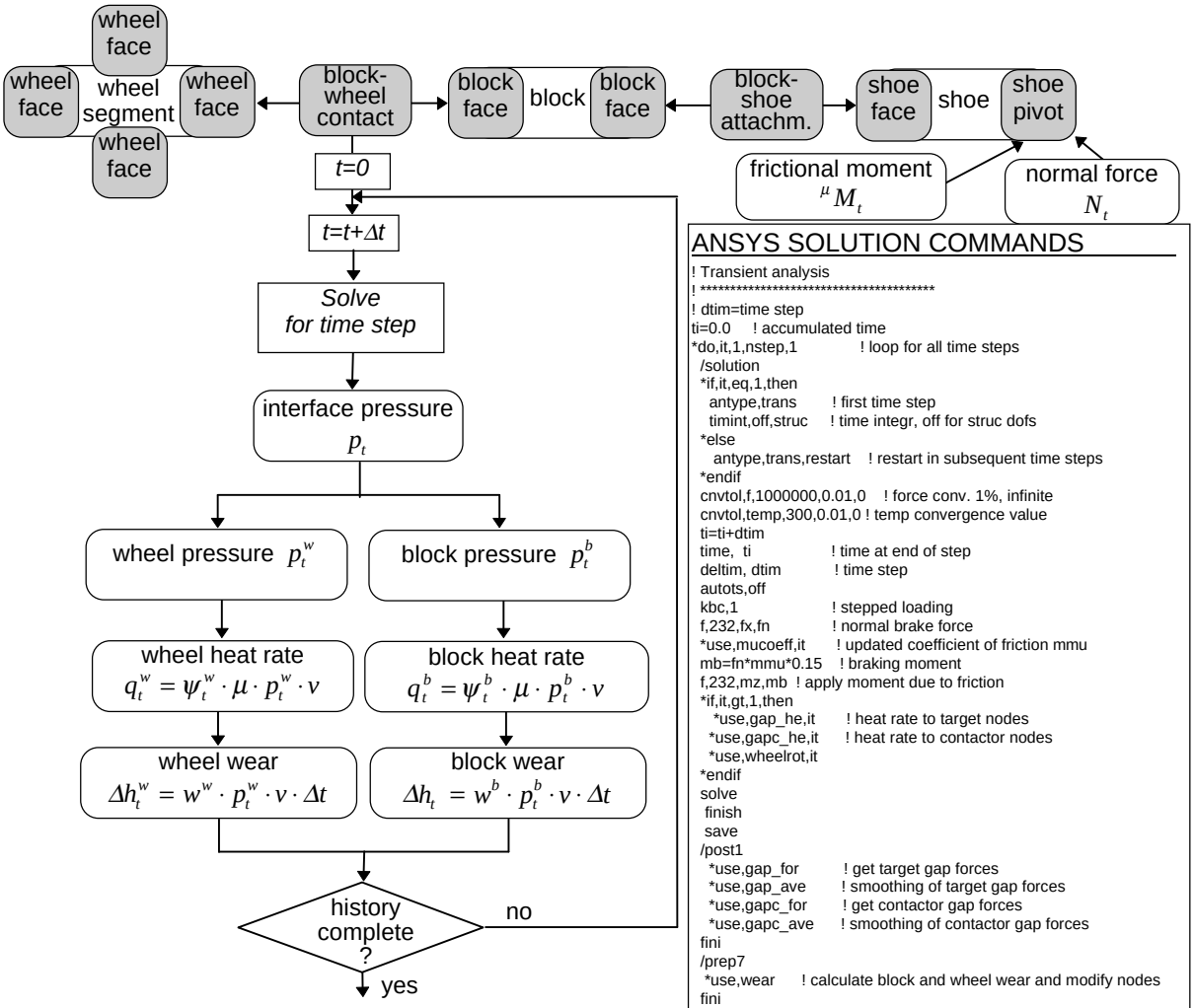

Figure 12. The simulation approach and a log of ANSYS solution commands.

Oscillation in the normalized contact pressure, due to the polygon effect introduced by the linear isoparametric elements, between a fully conform UIC250 block made of cast iron and a steel wheel with a diameter of 0.92m, is shown in figure 13A. The wheel element length is 0.89 mm and the block element length is 1.25 mm. Figure 13B shows the contact pressure distribution after three point smoothing according to equation 24. There are 100 elements for half a wavelength, i.e. 250 mm, and the error induced by a three point smoothing is negligible.

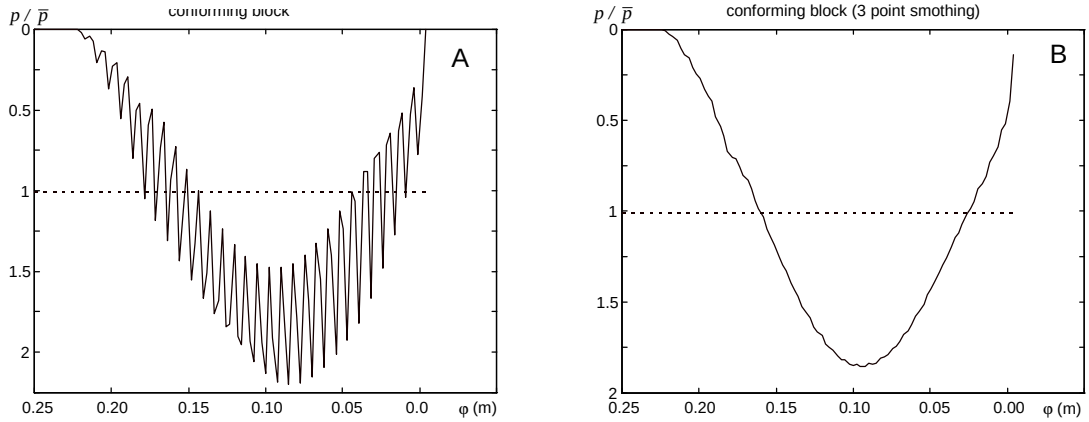

Figure 13. Pressure oscillation between block and wheel (A) and pressure after smoothing (B).

FE SIMULATION RESULTS

Three simulation cases are presented below. The first case, which is a collection of two simulations that can not be related to braking conditions found in the real world, can be characterized as synthetic case. It shows though some fundamental properties of a standard cast iron brake block. The second and third cases represent variations of a realistic braking condition. In these simulations, a force equivalent to a nominal contact pressure of 1 MPa, i.e. about twice the nominal pressure in normal stop braking, was used. The total frictional heating was applied as thermal loads on the target nodes on the block and the contactor nodes on the wheel tread.

In all presented simulations, the heat rate was calculated according to equation (1) and distributed to the nodes in an ANSYS macro that was called in each time step. The partitioning of the generated heat flow in the interface was solved implicitly by using a thermal conductance of 100 W/C for each contact element. The wheel was turned with an incremental sliding of 0.9 mm per time step.

Synthetic case

The synthetic case represent two simulations that were performed with physical data that can not be related to real world conditions. The velocity in these three simulations was 0.2 km/h, which correspond to a Peclet number slightly above 2.5, but the frictional heat rate was 300 times higher than a physically reasonable value, i.e. the heat rate corresponded to sliding at 60 km/h. The nominal braking pressure was 4 MPa, which also is higher than in normal stop braking. The block radius was chosen equal to the wheel radius, i.e. the contact was perfectly conform when braking started. These simulations show some fundamental properties of a standard cast iron brake block.

In the first simulation, no wear was integrated. Due to the initial parabolic pressure distribution and a high frictional heat rate, the thermoelastic effect in the block was strong enough to cause a rapid and large reduction of the contact zone (see figure 14 and 15). After approximately 20 mm of sliding the size of the contact zone and thus the pressure distribution reached steady state. The steady state width of the contact zone was a function of both the applied force and the mean heat rate. A larger force slightly increase the contact width and an increased heat rate has a decreasing effect on the contact width.

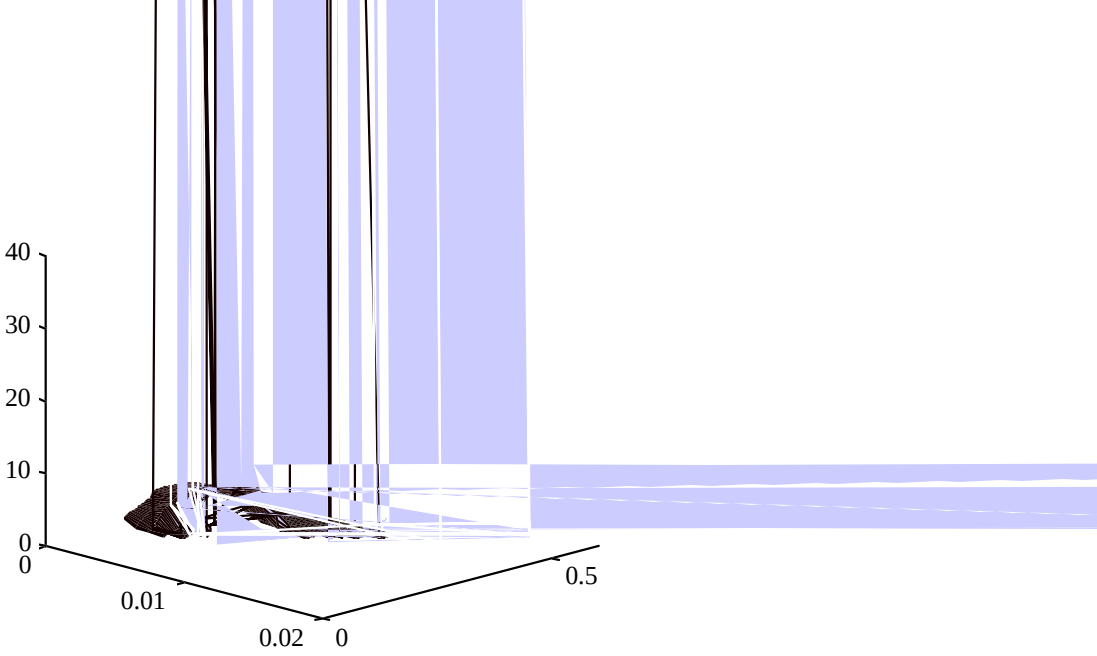
40
30
20
10
0
0
0.01
0.02
0
0.5

After about 2 cm of sliding, the maximum contact pressure continuously decreased because of the smoothening effect from wear. Figure 17A shows the pressure distribution between 45 mm and 60 mm of total sliding. After 60 mm of sliding, the contact patch has almost collapsed to two smaller patches. This phenomenon, which also is illustrated in figure 16B, is clearly caused by the block wear.

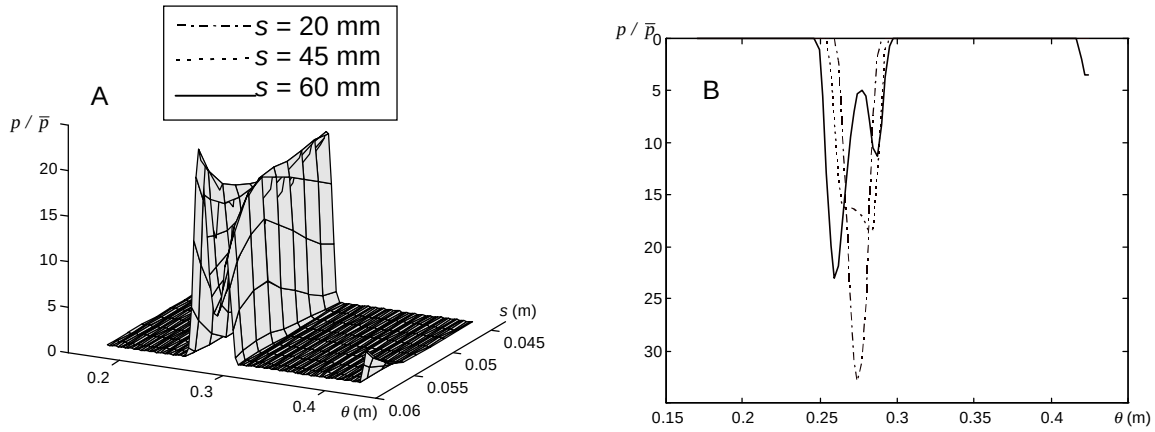

Figure 17. Pressure distribution normalized to the nominal pressure, as a function of sliding between 45 mm and 60 mm (A) and a "snap shot" of the pressure distribution at three time points (B).

Case 2 - Wear-in of a convex contact

In this case, all model and braking conditions have realistic values. The velocity is 60km/h, the nominal pressure is 1MPa, and a value of 0.2 was chosen for the coefficient of friction. A slightly convex contact was defined by giving the block a 5 mm larger radius than for the wheel (see figure 18A). Wear was included for the block. A wear coefficient w =3x10^{-12} Pa^{-1} was used. As an indication of a positive block wear, we can notice a slow increase of the length of the contact zone during the sliding history (see figure 18B).

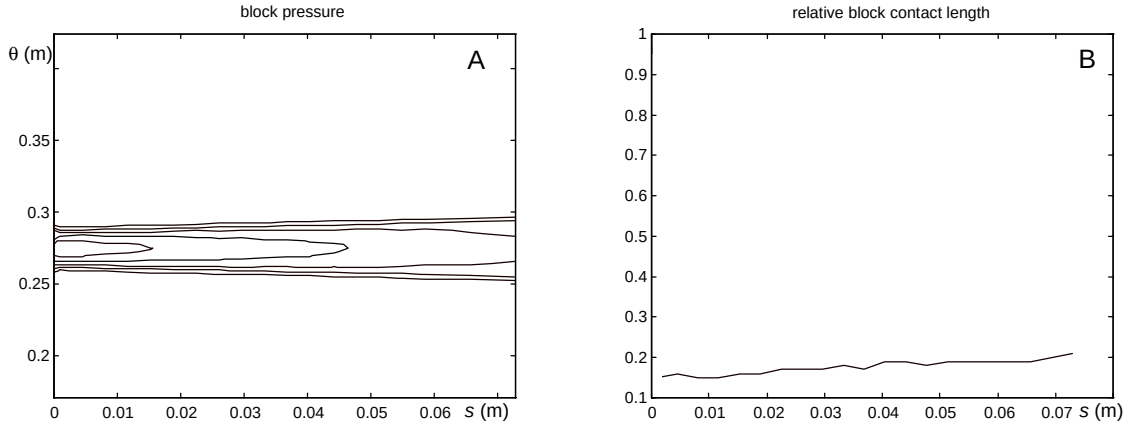

Figure 18. Pressure distribution (A) and normalized contact length (B) as a function of sliding distance.

After a sliding distance that equals the length of the contact zone, the maximum wheel temperature reaches an almost steady state value of 13C (see figure 19A). From the wheel temperature profiles in figure 19B we can notice a small oscillation of the wheel temperature that leaves the contact zone.

[redacted]

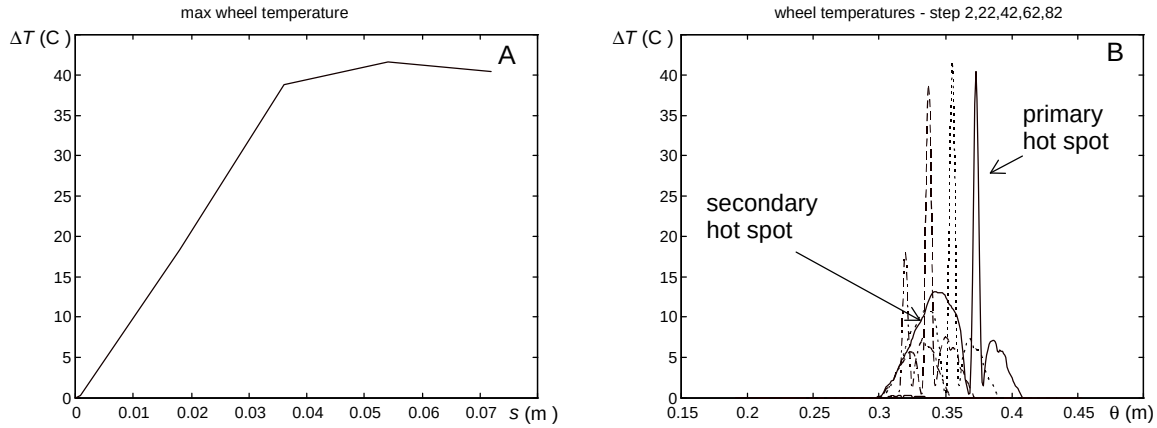

Figure 21. Maximum wheel temperature as a function of the sliding distance (A) and the wheel temperature distribution at five discrete time points (B).

CONCLUSIONS

FE simulations of TEI dominated phenomena require extraordinary computer resources. Discretization and time step constraints makes a 3D approach unrealistic in most cases. A 2D approach has been used to study the initiation of wheel corrugation due to braking on the tread with blocks made of cast iron.

Results from the FE simulations show that an initial pressure variation between block and wheel will grow exponentially during braking and the initial contact zone will be transformed to a limited number of separated contact patches due to TEI. Longer wavelength undulations, i.e. same order as the length of the contact patch, will become unstable before the short ones and thereby dominate the process. The process is very fast and may well be established on the wheel surface during the initial contact with a block.

For a rough and imperfect wheel surface, i.e. a real engineering surface, the roughness spectra will be transformed in the contact zone. The transformation depend on the material properties of the block as well as the actual design of the block.

The transformation of the wheel roughness during braking can be optimized or controlled by modifying the block material or the design. These parameters can be studied with the presented FE model.

ACKNOWLEDGMENT

The supervision of Professor Sören Andersson is gratefully acknowledged. This work was funded by the European Union and performed within the BRITE-EURAM III project no. BRPR-CT95-00 70 EUROSABOT.

REFERENCES

ANSYS, 1995, " ANSYS Theory Reference Manual, Release 5.2", Ed. Kohnke, P., ANSYS Inc.

Archard, J.F., 1953, ”Contact and rubbing of flat surfaces”, J. of Applied Physics, 24, pp. 981-988.

Archard, J.F., 1959, ”The temperature of rubbing surfaces”, Wear,2 , pp. 438-455.

Barber, J.R., 1967, "The influence of thermal expansion on the friction and wear processes", Wear, 10, pp. 155-159.

Burton, R.A., 1980),”Thermal deformation in frictionally heated contact”, Wear, 59, pp. 1-20.

Dings, P.C., 1994, "Rail roughness, rail transverse profile and noise, part 2 of SVV-project 1:Rolling noise, reduction of roughness" (in Dutch), NS Technical Research report no. CTO/7/10.448/0021.

Dittrich, M.G., Biegstraaten, F.J.W., Dings, P.C., and Thompson, D.J., 1994, "WHEEL ROUGHNESS AND RAILWAY ROLLING NOISE: THE INFLUENCE OF BRAKING SYSTEMS AND MILEAGE", Second International Symposium Transient Noise 94, St. Petersburg, Russia, October 4-6

Donea, J., 1974, ”On the accuracy of finite element solutions to transient heat conduction equations”, Int. J. Numer. Methods Eng., 8, pp. 103-110.

Dow, TH.A. and Burton, R.A., 1971, "Themoelastic instability of sliding contact in the absence of wear", Wear, 19, pp. 315-328.

Greenwood, J.A., 1991, ”An interpolation formula for flash temperatures", Wear, 150, pp. 153-158.

Guha, D. and Chowdhuri, S.K. Roy, 1996, ” The effect of surface roughness on the tmperature at the contct between sliding bodies”, Wear 197, 1996, pp. 63-73.

Hughes, T.J.R., 1977, " Unconditionally Stable Algorithms for Nonlinear Heat Conduction", Comp. Meth. Appl. Mech. Engng., 10 (2), pp. 135-139.

Johnson, K.L., 1994, "Contact mechanics", ISBN 0 521 34796 3, Cambridge University Press.

Rources, V. and Alarcon, E., 1983, ”Transient heat conduction problems using B.I.E.M.”, Comput. Struct., 16, pp. 717-730.

Sellgren, U., 1997, "Attachment of mating faces - an interrelational feature approach", Submitted for presentation at the 8th Int. ANSYS Conference.

Thompson, D.J., 1994, "PREDICTING RAILWAY ROLLING NOISE", Second International Symposium Transient Noise 94, St. Petersburg, Russia, October 4-6, pp.1-6.

Tian, X. and Kennedy, F.E., 1994, ” Maximum and Average Flash temperatures in Sliding Contacts”, Transactions of the ASME, Journal of tribology, Vol. 116, January 1994.

Vernersson, T., 1997, ”thermally Induced Roughness of tread Braked railway Wheels - a Noise-related Problem”, Thesis for the degree of Licentiate of Engineering, Chalmers University of technology, Division of Solid mechanics, ISSN 0283-8672 1997:4.